Diesel Exhaust Induces Systemic Lipid Peroxidation and Development of Dysfunctional Pro-Oxidant and Pro-Inflammatory High-Density Lipoprotein

Fen Yin, Akeem Lawal, Jerry Ricks, Julie R. Fox, Tim Larson, Mohamad Navab, Alan M. Fogelman, Michael E. Rosenfeld, Jesus A. Araujo

Objective—To evaluate whether exposure to air pollutants induces oxidative modifications of plasma lipoproteins, resulting in alteration of the protective capacities of high-density lipoproteins (HDLs).

Approach and Results—We exposed apolipoprotein E–deficient mice to diesel exhaust (DE) at ≈250 μg/m^3 for 2 weeks, filtered air (FA) for 2 weeks, or DE for 2 weeks, followed by FA for 1 week (DE+FA). DE led to enhanced lipid peroxidation in the brochoalveolar lavage fluid that was accompanied by effects on HDL functionality. HDL antioxidant capacity was assessed by an assay that evaluated the ability of HDL to inhibit low-density lipoprotein oxidation estimated by 2′,7′-dichlorofluorescein fluorescence. HDL from DE-exposed mice exhibited 23 053±2844 relative fluorescence units, higher than FA-exposed mice (10 282±1135 relative fluorescence units, $P<0.001$) but similar to the HDL from DE+FA-exposed mice (22 448±3115 relative fluorescence units). DE effects on HDL antioxidant capacity were negatively correlated with paraoxonase enzymatic activity, but positively correlated with levels of plasma 8-isoprostanes, 12-hydroxyeicosatetraenoic acid, 13-hydroxyoctadecadienoic acid, liver malondialdehyde, and accompanied by perturbed HDL anti-inflammatory capacity and activation of the 5-lipoxygenase pathway in the liver.

Conclusions—DE emissions induced systemic pro-oxidant effects that led to the development of dysfunctional HDL. This may be one of the mechanisms by which air pollution contributes to enhanced atherosclerosis. **(*Arterioscler Thromb Vasc Biol*. 2013;33:1153-1161.)**

Key Words: air pollution ■ diesel exhaust ■ dysfunctional high-density lipoproteins ■ oxidative stress

Downloaded from http://atvb.ahajournals.org/ by guest on December 26, 2016

Extensive epidemiological evidence supports the association of air pollution with adverse health effects, leading to increased cardiovascular morbidity and mortality of worldwide significance,[1] in particular of ischemic nature.[2] Although ambient air pollutants are a complex mixture of compounds with both gaseous and particle phases, epidemiological data and work with experimental animals support a causal association between the particulate matter (PM) components and atherosclerosis.[1,3] For example, exposure of Watanabe hyperlipidemic rabbits to intratracheal PM_{10} (PM<10 μm)[4] or apolipoprotein E–deficient (apoE$^{-/-}$) mice to inhaled fine particulates ($PM_{2.5}$<2.5 μm)[5] resulted in enhanced atherosclerosis. It seems that PM proatherogenic actions are linked to their ability to elicit systemic pro-oxidative and proinflammatory effects.[3] In addition, we have reported that ambient PM in the ultrafine-size range (PM<0.18 μm) enhanced aortic atherosclerosis to a larger degree than $PM_{2.5}$,[6] supporting the notion that the smallest particulates could lead to stronger cardiovascular effects.[7] Moreover, although normal high-density lipoprotein (HDL) can protect against pro-oxidant effects induced by air pollutant organic chemicals in endothelial cells and macrophages,[8] both fine and ultrafine ambient PM lead to the development of dysfunctional HDLs that lose their anti-inflammatory properties.[6]

Although the sources of air pollution are heterogeneous, emissions from gasoline and diesel-powered motor vehicles are major contributors in urban settings. Indeed, diesel exhaust (DE) emissions are characterized by a large number of ultrafine particles, rich in organic content, such as polycyclic aromatic hydrocarbons. Exposure of apoE$^{-/-}$ mice to total DE resulted in atherosclerotic plaques with enhanced oxidative stress,[9] increased cellularity,[9] and larger macrophage content[10] that could, in the setting of human atherosclerosis, suggest a greater propensity for rupture. Although the accrued experimental evidence supports the proatherogenic effects of ambient PM, the mechanisms by which the inhalation of air pollutants are transduced systemically and lead to adverse vascular effects are not well understood. We have hypothesized that PM-induced

Received on: September 27, 2012; final version accepted on: February 10, 2013.

From the Department of Medicine, Division of Cardiology, David Geffen School of Medicine, University of California, Los Angeles, CA (F.Y., A.L., M.N., A.M.F., J.A.A.); and Department of Environmental and Occupational Health Sciences (J.R., J.R.F., T.L., M.E.R.) and Department of Civil and Environmental Engineering (T.L.), University of Washington, Seattle, WA.

The online-only Data Supplement is available with this article at http://atvb.ahajournals.org/lookup/suppl/doi:10.1161/ATVBAHA.112.300552/-/DC1.

Correspondence to Jesus A. Araujo, MD, PhD, University of California, Los Angeles, Division of Cardiology, 10833 Le Conte Ave, CHS 43-264, Los Angeles, CA 90095. E-mail JAraujo@mednet.ucla.edu

© 2013 American Heart Association, Inc.

alterations in HDL may be associated with or are the result of systemic pro-oxidant effects, and that changes in HDL function mediate some of the PM-induced proatherogenic responses. Although plasma levels of HDL cholesterol have been shown to be inversely correlated with atherosclerosis and ischemic heart disease,[11,12] high HDL cholesterol levels may not always be protective,[13] and genetic mechanisms that raise plasma HDL cholesterol do not lower risk of myocardial infarction,[14] which suggests that HDL composition and functional aspects may be even more important than the levels of HDL cholesterol. In addition, different HDL protective qualities may correlate with different outcomes. Thus, the reverse cholesterol transport function of HDL inversely associates with carotid intima-media thickness and the likelihood of angiographic coronary artery disease,[15] whereas the antioxidant function of HDL was significantly impaired in subjects with acute coronary syndromes as compared with healthy subjects or those with stable coronary artery disease.[16]

In the current study, we aimed to determine whether 2-week inhalation exposures of mice to DE emissions could induce alterations in HDL antioxidant capacity similar to the way that 5-week inhalation of concentrated ambient particles resulted in the development of dysfunctional pro-inflammatory HDL[6] and to determine whether the alterations in HDL are associated with and attributable to DE pro-oxidative effects in systemic tissues and plasma lipoproteins. In addition, we explored the potential reversibility of the DE-induced effects.

Materials and Methods

Materials and Methods are available in the online-only Supplement.

Results

Exposure to Diesel Emissions Results in Loss of Plasma HDL Anti-Inflammatory Properties

We conducted 2 inhalation experiments on mice (Figure 1A). In experiment 1, we explored whether inhalation exposures to DE would alter HDL anti-inflammatory capacity as did concentrated ambient particles.[6] Nine-week-old male apoE null mice were assigned to 3 groups (n=12–13/group) that were exposed to the following: (1) DE for 2 weeks (DE group), (2) filtered air (FA) for 2 weeks (FA) as controls, and (3) DE for 2 weeks followed by FA for 1 additional week (DE+FA). The purpose of the DE+FA group was to assess the reversibility of DE-induced changes after 1 week of additional FA exposures (Figure 1A). DE exposures consisted of total DE at ≈250 μg/m^3 of $PM_{2.5}$ (PM diameter <2.5 μm) mass in a Biozone unit at the Northlake exposure facility. Exposure parameters are mentioned in the online Material and Methods in the online-only Data Supplement. The DE particle mass size distribution corresponding to all experiments is shown in Figure 1B. To test the HDL anti-inflammatory capacity, we used a monocyte chemotaxis assay that evaluates the ability of HDL to inhibit low-density lipoprotein (LDL)–induced monocyte migration in a vascular cell coculture system.[17] Although plasma HDL from the FA controls inhibited LDL-induced monocyte migration, plasma HDL from DE and DE+FA mice did not protect but induced significantly more monocyte migration than LDL alone. This indicates that the HDL had become proinflammatory (Figure 2A). The proinflammatory properties were not attributable to a gain of serum amyloid A because there were no significant changes in serum amyloid A levels (data not shown).

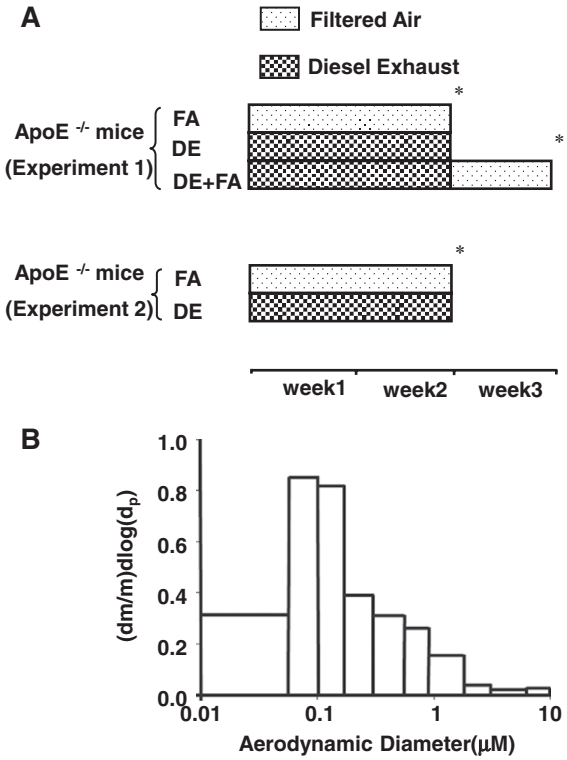

Figure 1. Diesel exhaust (DE) exposures. **A**, Experimental protocol. Three groups of male apolipoprotein E (apoE) null mice (experiment 1) were exposed to filtered air (FA) for 2 weeks, DE for 2 weeks (DE), and DE for 2 weeks followed by FA for 1 additional week (DE+FA). In experiment 2, apoE null mice were exposed to FA vs DE. *Time at which mice were bled and euthanized, and tissue harvesting was performed. **B**, Particle mass and size. Typical particle mass and size distribution of DE measured at a $PM_{2.5}$ concentration of 217 μg/m^3. In this case, the mass median aerodynamic diameter was 77 nm, and the count median thermodynamic equivalent diameter was 87 nm, indicating that a large portion of DE particles are in the ultrafine-size range. d indicates derivative; dp, particle diameter; m, mass; and PM, particulate matter.

DE Exposures Also Lead to Alteration of HDL Antioxidant Function

To assess HDL antioxidant capacity, we used a cell-free assay that evaluates the ability of HDL to inhibit LDL oxidation measured by 2′,7′-dichlorofluorescein (DCF) fluorescence.[8] Mice exposed to DE (DE and DE+FA groups) exhibited significantly higher levels of DCF fluorescence as compared with FA controls (Figure 2B). Interestingly, there were no differences between the DE and DE+FA groups. We generated an HDL Oxidant Index (HOI) by normalizing the DCF fluorescence in the presence of HDL by the fluorescence developed in its absence. Although all of the mice from the DE (2.21±0.27) and DE+FA groups (2.10±0.25) displayed an HOI>1.0, indicative of pro-oxidative HDL, 10 of 13 mice exhibited HOI<1.0 in the FA group (0.94±0.12; Figure 2C). Thus, a 2-week exposure to DE significantly induced

Downloaded from http://atvb.ahajournals.org/ by guest on December 26, 2016

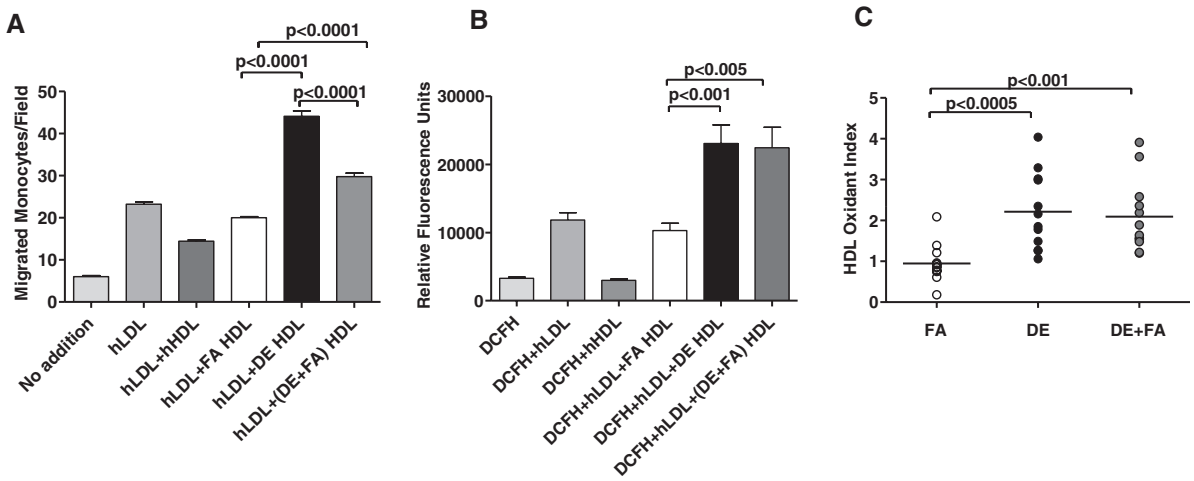

Figure 2. Diesel exhaust (DE) leads to dysfunctional high-density lipoprotein (HDL). **A**, HDL anti-inflammatory capacity. Pooled plasma HDL from filtered air (FA; n=4), DE (n=3), and DE+FA mice (n=4) was added to cocultures of human aortic endothelial and smooth muscle cells in the presence of human low-density lipoprotein (LDL). Values are expressed as mean±SEM of the number of migrated monocytes/field in 9 fields. **B**, HDL antioxidant capacity expressed by DCF relative fluorescence intensity. Plasma HDL from FA (n=13), DE (n=12), and DE+FA mice (n=13) was tested by a cell-free assay method. Values are expressed as the mean±SEM of relative fluorescence units. **C**, HDL Oxidant Index (HOI) calculated as described in the online Materials and Methods in the online-only Data Supplement. Group averages are indicated by straight horizontal bars. DCFH indicates 2′,7′-dihydrodichlorofluorescein; hHDL, human HDL; and hLDL, human LDL.

Downloaded from http://atvb.ahajournals.org/ by guest on December 26, 2016

the generation of dysfunctional pro-oxidative HDL that remained as such after 1 week of additional FA inhalation. Although these results paralleled the loss of anti-inflammatory protection in the DE mice (Figure 2A), the level of DCF fluorescence remained elevated in the DE+FA group but the degree of monocyte migration in the DE+FA group was lower as compared with the DE group ($P<0.0001$), suggesting that the kinetics of recovery of HDL anti-inflammatory properties, although only partial, was faster than that of the HDL antioxidant capacity (Figure 2). Changes in HDL functionality occurred without influencing HDL cholesterol levels (Table I in the online-only Data Supplement), plasma lipoproteins fast protein liquid chromatography profile (Figure I in the online-only Data Supplement), or HDL ability to promote cholesterol efflux (Figure II in the online-only Data Supplement).

DE-Induced Dysfunctional HDL Is Associated With Decreased Paraoxonase Activity and Increased Lipid Peroxidation

We first explored whether DE actions on HDL function could have been attributable to enhancement of myeloperoxidase activity in the blood, but there were no significant differences in myeloperoxidase activity between groups (Figure III in the online-only Data Supplement). We then hypothesized that DE may lead to changes in paraoxonase 1 (PON1) that could alter its enzymatic activity, known to provide an important contribution to HDL-mediated antioxidant protection.[18] In support of our hypothesis, plasma PON1 activity was significantly decreased in DE mice as compared with FA controls (Figure 3A) despite the presence of similar levels of PON1 mRNA in the liver (Figure IVA in the online-only Data Supplement). There was a trend for a negative correlation between PON1 activity and HOI ($r=-0.2197$; $P=0.19$) that was statistically significant when the DE+FA mice were excluded ($r=-0.392$; $P=0.05$; Figure 3B), suggesting that changes in PON1 activity may account for some of the HDL effects in only the DE group. In addition, we observed an increase in plasma levels of 8-isoprostanes, one of the products of lipid peroxidation, in both DE and DE+FA mice (Figure 3C), and a positive correlation with the HOI ($r=0.741$; $P<0.0001$; Figure 3D). Furthermore, we found that as compared with FA controls, mice from the DE and DE+FA groups exhibited 2- to 3-fold increases in the plasma levels of 12-hydroxyeicosatetraenoic acid (12-HETE) and 13-hydroxyoctadecadienoic acid (13-HODE), peroxidation products of arachidonic and linoleic fatty acids, respectively (Figure 3E and 3G). There were also strong correlations between the plasma levels of 12-HETE, 13-HODE, and the HOI ($P<0.001$; Figure 3F and 3H). Because increased peroxidation in plasma lipoproteins may not only involve HDL lipoproteins but also other non-HDL fractions, such as LDL, intermediate-density lipoprotein, or very low density lipoproteins (VLDL), we assessed the degree to which apoB-containing lipoproteins were susceptible to oxidation by DCF fluorescence. Mice from the DE group exhibited non-HDL lipoproteins that were more oxidizable than those from the FA controls ($P<0.05$; Figure V in the online-only Data Supplement). In contrast, 1 week of FA exposures after DE was sufficient to reduce the oxidation capacity of non-HDL lipoproteins that tended to be lower than that of the DE group ($P=0.12$).

DE Leads to Increased Lipid Peroxidation in the Bronchoalveolar Compartment and in Systemic Tissues

We hypothesized that the lungs would be the logical source for the increased oxidized lipids in the plasma. Surprisingly, there were no changes in the levels of malondialdehyde (Figure 4A) or increases in HETEs/HODEs in whole lung homogenates (Table II in the online-only Data Supplement). However, we did observe an increase of almost 4-fold in the levels of 12-HETE ($P<0.05$; Figure 4B, Table) and a borderline significant trend toward increased levels of 13-HODE ($P=0.06$;

Table. Tissue and BALF Levels of HETEs and HODEs†

	FA	DE	DE+FA
Plasma, ng/mL‡			
5-HETE	ND	ND	ND
12-HETE	936.9±185.0	1845.1±361.4*	1873.8±241.5**
15-HETE	ND	ND	ND
9-HODE	4.08±0.52	4.30±0.80	4.89±0.22
13-HODE	6.69±2.32	15.3±2.83*	18.0±1.46**
Liver, ng/g tissue§			
5-HETE	10.6±3.70	56.9±17.0*	25.3±10.1
12-HETE	111.1±38.0	119.1±14.0	102.9±13.4
15-HETE	84.1±8.13	93.7±14.7	108.4±7.05
9-HODE	1413.7.5±130.1	1304.2±150.3	1365.3±49.8
13-HODE	1247.5±192.7	989.1±188.7	1357.8±105.8
Large intestine, ng/g tissue‖			
5-HETE	21.1±2.83	125.9±24.9*	…
12-HETE	503.8±55.3	600.9±91.5	…
15-HETE	897.6±38.9	1022.4±103.9	…
9-HODE	8353.2±336.8	6535.7±950.5	…
13-HODE	4493.2±86.1	4501.0±54.1	…
BALF, ng/mL¶			
5-HETE	ND	ND	…
12-HETE	3.3±1.5	12.2±3.2*	…
15-HETE	ND	1.4±0.1*	…
9-HODE	0.8±0.2	1.8±0.5	…
13-HODE	4.6±0.5	9.6±2.4#	…

DE indicates diesel exhaust; FA, filtered air; HETE, hydroxyeicosatetraenoic acid; HODE, hydroxyoctadecadienoic acid; and ND, not detected.

†Results are expressed as mean±SEM.

‡n=5 for each group.

§n=5 for FA and DE+FA; n=6 for DE group.

‖n=5 for FA and n=3 for DE group.

¶n=5 for each group.

‡,§ correspond to experiment 1.

‖,¶ correspond to experiment 2.

*P<0.05 vs FA group.

**P<0.005 vs FA group. #P=0.06.

Figure 4B; Table) in the presence of similar bronchoalveolar lavage total protein (Figure 4C). This mirrored similar effects seen in the plasma. In addition, as compared with FA controls, DE mice exhibited greater levels of 5-HETE (P<0.05; Figure 4D) and MDA (P<0.05; Figure 4E) in the liver, and there was a positive correlation between liver MDA and plasma HOI (Figure 4F). Similarly, DE led to increased levels of 5-HETE in the intestines (Table).

DE Activates the 5-lipoxygenase Pathway in the Liver

The singular increase in hepatic 5-HETEs suggested specific activation of the 5-lipoxygenase pathway in the liver (Figure 5A). This was supported by the DE-induced significant upregulation of the arachidonate 5-lipoxygenase mRNA (Figure 5B) and protein (Figure 5C) expression, together with increased mRNA expression of glutathione peroxidase 6 (Figure 5B), but no significant differences in arachidonate 12-lipoxygenase or arachidonate 15-lipoxygenase mRNA expression (Figure IVB and IVC in the online-only Data Supplement). Increased lipid peroxidation in the liver led to triggering of an antioxidant response as evidenced by the upregulation not only of glutathione peroxidase 6, but also of NAD(P)H-quinone oxidoreductase 1 (79-fold), the catalytic subunit of glutamate cysteine ligase (6.2-fold) and superoxide dismutase 1 (2.1-fold). There was also upregulation of activating transcription factor 4 (4.9-fold), an important component of one of the branches of the unfolded protein response (Figure 5C). DE+FA group also exhibited upregulation of the first 4 genes but no differences in superoxide dismutase 1 levels as compared with FA controls, suggesting that the transcriptional regulation of various antioxidant genes had different kinetics.

Discussion

Our study reveals that a 2-week exposure to DE leads to systemic pro-oxidative effects characterized by increased lipid peroxidation and alteration of HDL protective capacities.

This extends our previous study where 5-week exposure of apoE$^{-/-}$ mice to ultrafine ambient particles led to enhanced atherosclerosis and the development of dysfunctional proinflammatory HDL[6] by demonstrating: (1) modifying effects of the direct inhalation of motor vehicle emissions, considered to be an important contributor to air pollution in cities, on HDL antioxidant as well as anti-inflammatory properties, (2) DE induction of various lipid peroxidation products in the BALF, plasma, and systemic tissues, such as the liver and intestines, and (3) activation of the 5-lipoxygenase pathway in the liver. Our findings are consistent with epidemiological studies that have found associations between exposure to ambient particulate PM and measures of systemic oxidative stress that include biomarkers of oxidative alteration of proteins, lipids, and DNA in the circulating blood or in products excreted in the urine.[3,19]

DE-induced pro-oxidative effects were indicated by increased lipid peroxidation[20] that in the blood and in the liver correlated with the HOI (Figure 3). This suggests that alterations in HDL functions are likely associated with HDL oxidative modifications. For example, mice from the DE and DE+FA groups exhibited increased plasma levels of 8-isoprostanes, which are formed by nonenzymatic free radical–mediated oxidation of arachidonic acid and have been regarded as a gold standard in the assessment of lipid peroxidation and oxidative stress.[3,20] Although we did not measure 8-isoprostanes in the HDL fraction but only in whole plasma, HDL has been reported to be the major lipoprotein carrier of 8-isoprostanes in human plasma, with levels that are significantly higher than in LDL or VLDL.[21] It is likely that increased plasma levels of 8-isoprostanes in mice also reflect an increased content in the HDL particles. However, we also found increased susceptibility to oxidation of apoB-containing lipoproteins from the DE mice (Figure V in the online-only Data Supplement), and this suggests that lipid peroxidation products could also be seeding particles from the VLDL and LDL size fractions. DE-induced 8-isoprostanes in the blood could originate from the peroxidation of arachidonic acid in plasma lipoproteins but they could also derive from lipid peroxidation occurring in systemic tissues. Our results are consistent with the study by Bai et al[9] who

Downloaded from http://atvb.ahajournals.org/ by guest on December 26, 2016

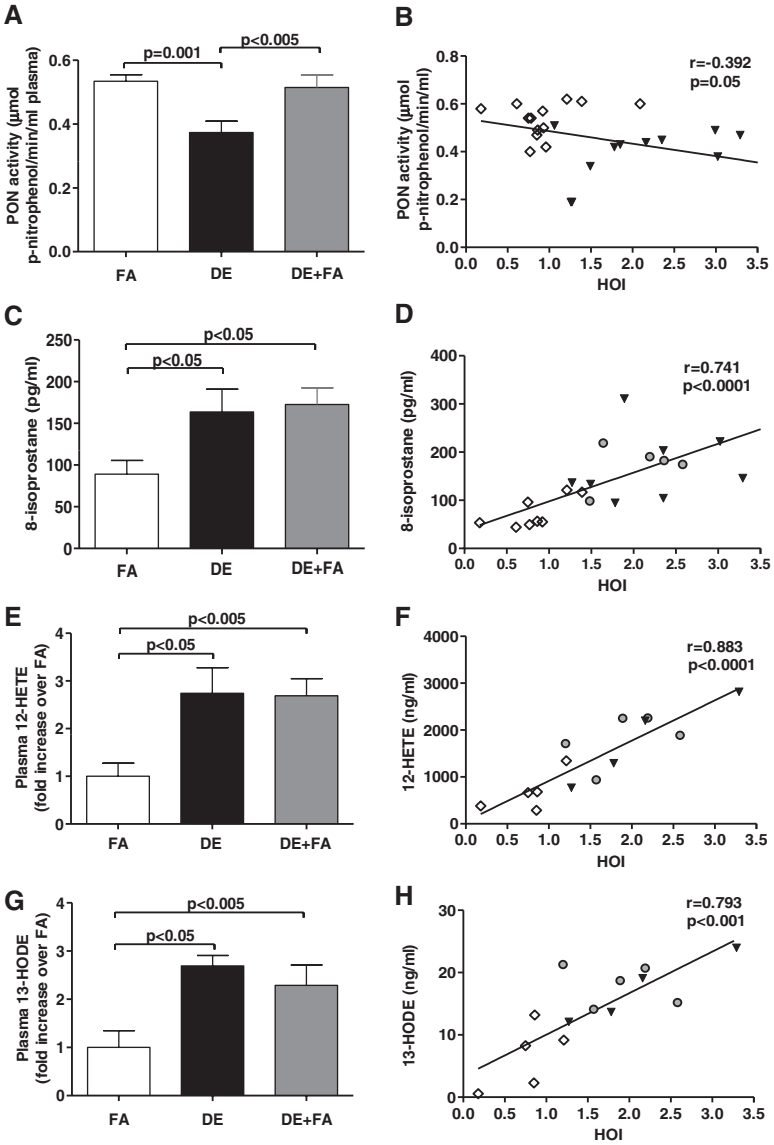

Figure 3. Diesel exhaust (DE) exposures lead to plasma enzymatic and lipid alterations. Plasma paraoxonase activity (**A**), plasma 8-isoprostane levels (**C**), plasma levels of 12-hydroxyeicosatetraenoic acid (12-HETE; **E**) and 13-hydroxyoctadecadienoic acid (13-HODE; **G**). Correlations of plasma paraoxonase activity (**B**), 8-isoprostane (**D**), 12-HETE (**F**), and 13-HODE (**H**) with High-Density Lipoprotein Oxidant Index (HOI) in mice from the filtered air (FA; empty rhomboids), DE (filled triangles), and DE+FA (gray circles) mice. n= 5 to 10/group.

Downloaded from http://atvb.ahajournals.org/ by guest on December 26, 2016

showed that DE exposure of apoE$^{-/-}$ mice in the same facility resulted in increased levels of 8-isoprostane and 8-hydroxydeoxyguanosine levels in the urine and significantly extends it, by providing direct evidence of increased lipid peroxidation in the plasma together with alteration of HDL functions.

DE exposure also led to increased levels of other peroxidation products in the blood, derived from polyunsaturated fatty acids, such as 12-HETEs and 13-HODEs[22,23] (Table). We hypothesized that DE exposures may have induced oxidative modifications of HDL particles that could have resulted in alterations of antioxidant enzymes associated with HDL, modifications in HDL architecture or changes in apoA1, leading to a decreased ability to inhibit oxidation. Previous reports have shown that increased plasma–oxidized phospholipids associate with decreased activity of PON1, platelet-activating factor acetylhydrolase (also known as lipoprotein-associated phospholipase A2), and lecithin-cholesterol-acyltransferase in apoE$^{-/-}$ mice,[24] but it is not clear whether those associations were causal. Although we did not assess platelet-activating factor acetylhydrolase or lecithin-cholesterol-acyltransferase, we did observe that mice exposed to DE exhibited decreased PON1 activity, likely as a result of post-translational modifications because there were no differences in hepatic PON1 mRNA expression (Figure IVA in the online-only Data Supplement). This has also been shown to occur in oxidized HDL,[25,26] resulting in decreased protection against lipid oxidation in LDL and cell membranes.[26] However, the lack of recovery in the HDL antioxidant capacity in the DE+FA mice suggests that other factors must be responsible for the persistent alteration noted in this group. In addition to changes in antioxidant enzymes, it is possible that HDL nonenzymatic components with antioxidant properties, such as apoA1,[27] could have been altered. For instance, aldehydes derived from lipid peroxidation could also modify such proteins, similar to the way MDA has been shown to modify apoA1.[28] Thus, DE exposures led to increased levels of MDA and oxidative stress in the liver (Figures 4 and 5), which is consistent with our previous findings in apoE$^{-/-}$ mice exposed to ambient ultrafine particles.[6,29] Although liver MDA strongly associated with the HOI, it is unknown whether this association was causal. DE also led to activation of the

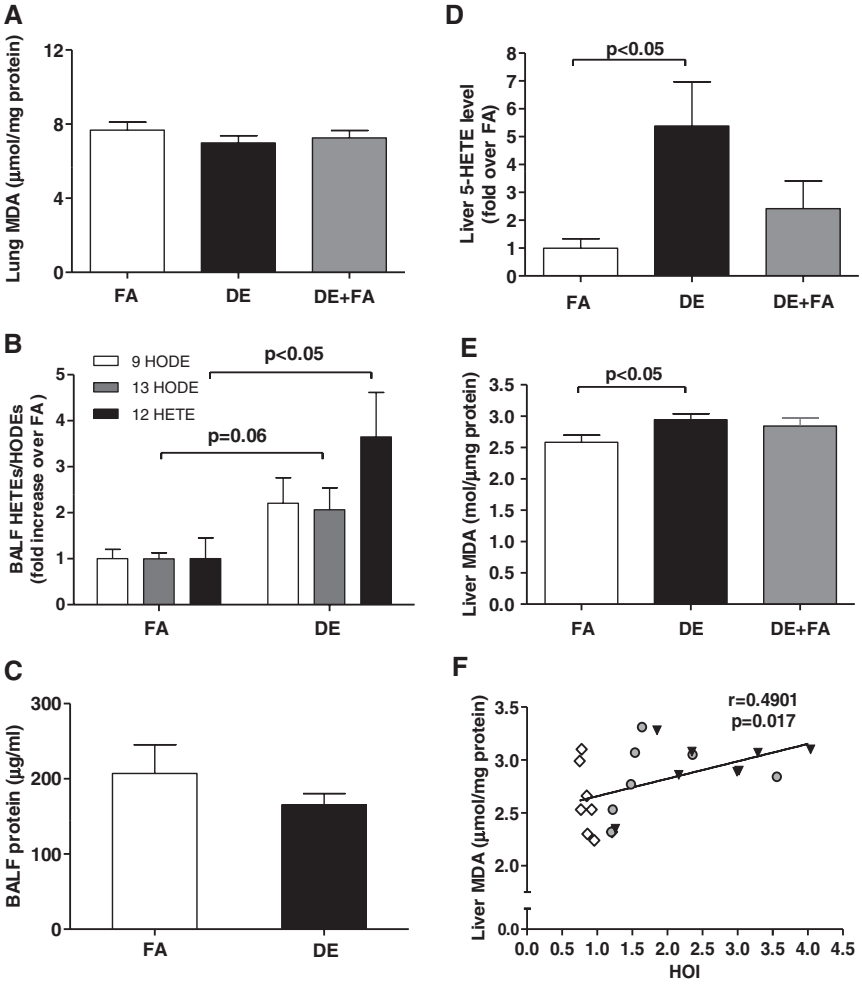

Figure 4. Diesel exhaust (DE) leads to increased lipid peroxidation in the BALF and in the liver. **A**, Lung MDA, (**B**) BALF hydroxyeicosatetraenoic acid (HETEs)/hydroxyoctadecadienoic acid (HODEs), expressed as fold changes over filtered air (FA) controls. **C**, BALF total protein. **D**, Liver 5-HETE levels, expressed as fold changes over FA controls (n=5/group). **E**, Liver MDA levels. **F**, Correlation of liver MDA and High-Density Lipoprotein Oxidant Index (HOI). Data in (**A** and **D**–**F**) correspond to experiment 1, and data in (**B** and **C**) correspond to experiment 2.

5-lipoxygenase pathway in the liver as evidenced by increased expression of arachidonate 5-lipoxygenase and glutathione peroxidase 6, which resulted in increased levels of 5-HETEs (Figure 5). Interestingly, DE-induced 5-HETEs were also noted in the intestines but not in the blood (Table) or the lungs (Table II in the online-only Data Supplement). This raises the possibility that part of the DE could have entered the body through the gastrointestinal tract. Additional studies will be required to determine the importance of this potential port of entry in the inhalation exposures to DE.

One putative mechanism for how the inhalation of motor vehicle emissions contributes to systemic inflammation is via the release of inflammatory mediators from the lungs into the systemic circulation. Surprisingly and unlike in the liver, we did not observe any DE-induced pro-oxidative effects on the levels of MDA, HETEs, and HODEs in whole lung homogenates or proinflammatory effects on the levels of BALF total protein. This is consistent with the study of Tong et al where intratracheal administration of ultrafine particles resulted in enhanced cardiac ischemia/reperfusion injury in the absence of any significant pulmonary inflammatory responses.[30] However, we did observe increased levels of 12- and 15-HETE ($P<0.05$) and an almost significant trend for greater levels of 13-HODE ($P=0.06$) in the BALF (Figure 4B), which supports the notion that DE can induce lipid peroxidation in the bronchoalveolar space that may contribute to the increased oxidized lipids in the circulating blood. DE-induced oxidative products in the BALF suggest obviation of the surfactant barrier function, perhaps resulting in exposure of lipoproteins to the DE or oxidative products induced in the alveolar-capillary unit. This is consistent with the report of Kampfrath et al[31] that inhalation of concentrated $PM_{2.5}$ led to increased oxidized phospholipid derivatives of 1-palmitoyl-2-arachidonyl-*sn*-glycero-3-phosphorylcholine in the BALF, that depended on toll-like receptor 4 signaling and NADPH oxidase activation. Interestingly, HDL has been reported to inhibit lipopolysaccharide-induced activation of macrophage inflammatory genes that are toll-like receptor 4-dependent, specifically via inhibition of the TRAM/TRIF pathway, independently of its effects on sterol metabolism.[32] This is important because DE-induced changes in the antioxidant and anti-inflammatory functions, but not in its reverse cholesterol transport capability, are consistent with the associations reported in human subjects between various cardiovascular end points and different functional aspects of HDL.[15,16] In addition, we have recently shown that although normal HDL can inhibit the oxidation of DE particles organic chemicals and DE particles pro-oxidative effects in endothelial cells and macrophages, dysfunctional HDL further induces, rather than inhibits, DE particles oxidation.[8]

Downloaded from http://atvb.ahajournals.org/ by guest on December 26, 2016

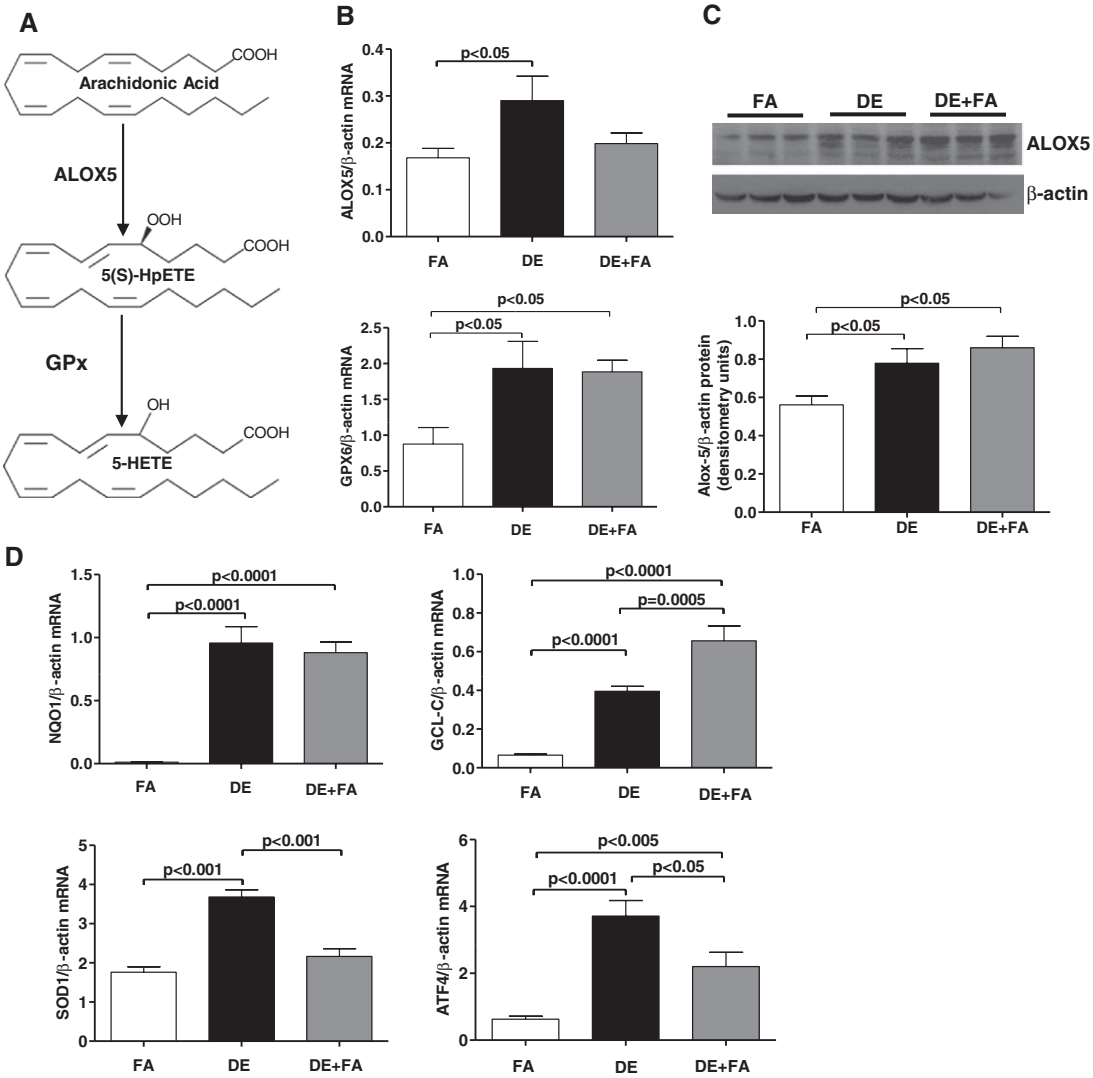

Figure 5. Diesel exhaust (DE) activates 5-LPO pathway in the liver. **A**, Schematics indicating oxidation of arachidonic acid into 5-hydroxyeicosatetraenoic acid (5-HETE). **B**, Arachidonate 5-lipoxygenase (ALOX-5) and glutathione peroxidase 6 (Gpx6) mRNA gene expression, (**C**) ALOX-5 protein expression; (**top**) Western immunoblot, (**bottom**) densitometric analyses, based on n=5/group. **D**, Antioxidant genes. Gene expression levels were determined by quantitative polymerase chain reaction in the livers of filtered air (FA), DE, and DE+FA mice (n=7/group). Values are expressed as the mean±SEM of mRNA levels normalized by β-actin mRNA. ATF4 indicates activating factor 4; GCL-C, catalytic subunit of glutamate cysteine ligase; LPO, lipoxygenase; NQO-1, NAD(P)H-quinone oxidoreductase 1; and SOD1, superoxide dismutase 1.

Downloaded from http://atvb.ahajournals.org/ by guest on December 26, 2016

In this study, we did not determine which component(s) of the DE were responsible for the observed effects. However, DE emissions have a high content of particles in the ultrafine-size range (Figure 1B), which accounted for ≈48% (aerodynamic diameter <0.10 µm) of the total particulate mass and ≈55% of the number of particles (thermodynamic equivalent diameter <0.103 µm). Similarly, ≈68% of the total particle mass had diameters <0.17 µm, and ≈74% of the total number of particles had diameters <0.15 µm. The particle count size distribution of the DE in this investigation is consistent with aged ambient particles that have been measured near roads,[33–35] generally larger than the count size distribution of freshly emitted DE.[36] Therefore, 2-week exposures to DE may have reproduced the systemic pro-oxidative effects exerted by 5-week exposures to concentrated ultrafine particles likely because of their high content in ultrafines. Consistent with our previous report,[6] additional studies in mice have shown that inhalation of ambient PM for several weeks results in enhancement of atherosclerotic lesions,[3] and that exposure to DE leads to aortic atherosclerotic plaques with a greater macrophage content[10] and foam cell formation[9] that in human subjects could indicate a greater propensity for rupture. Indeed, exposure to $PM_{2.5}$, largely originating from diesel and gasoline emissions in cities, has been correlated with increased risk for cardiovascular events and mortality, to the extent that the associations reflect not only between-city effects but also within-city effects.[37]

In conclusion, this study provides the first evidence that inhalation exposure to total DE leads to alteration of the HDL antioxidant and anti-inflammatory properties in association with increased lipid peroxidation in plasma and systemic tissues as well as activation of the 5-lipoxygenase pathway in the liver. Future studies that include either pharmacological

or genetic interventions will be required to elucidate the precise mechanism(s) responsible for these effects. In addition, both epidemiological and experimental human studies will be important to determine the relevance of the DE-induced HDL alteration in human subjects.

Acknowledgments

We are thankful to Ladan Vakili and the Essential Laboratory Services Core from the University of California, Los Angeles (UCLA) Atherosclerosis Research Unit for providing human low-density lipoprotein, Greg Hough for assistance with the liquid chromatography–mass spectrometry (MS)/MS methodology, Alan Wagner for advice in the cholesterol efflux assays, and Aldons Lusis for constructive review of the article. We also acknowledge the UCLA Molecular Instrumentation Center for providing the mass spectrometric instrumentation for this work. James Stewart of the University of Washington (UW), Department of Environmental and Occupational Health Sciences and Timothy Gould of the UW Department of Civil and Environmental Engineering were also instrumental in generating and characterizing the diesel exhaust exposures.

Sources of Funding

This work was supported by the National Institutes of Environmental Health Sciences (ONES RO1 Award ES016959 to Dr Araujo, the University of Washington P50 ES015915 DISCOVER Center: Cardiovascular Disease and Traffic-Related Air Pollution for Dr. Rosenfeld, the Epidemiologic and Bioinformatic Training in Environmental Health Training grant ES015459 for Dr. Fox), the Environmental Protection Agency funded University of Washington Clean Air Research Center grant for Drs Larson and Rosenfeld, and the National Heart, Lung, and Blood Institute (PO1 HL 30568 to Dr Fogelman).

Disclosures

Drs Navab and Fogelman are principals in Bruin Pharma, and Dr Fogelman is an officer in Bruin Pharma. The other authors have no conflicts to report.

References

1. Brook RD, Rajagopalan S, Pope CA 3rd, Brook JR, Bhatnagar A, Diez-Roux AV, Holguin F, Hong Y, Luepker RV, Mittleman MA, Peters A, Siscovick D, Smith SC Jr, Whitsel L, Kaufman JD; American Heart Association Council on Epidemiology and Prevention, Council on the Kidney in Cardiovascular Disease, and Council on Nutrition, Physical Activity and Metabolism. Particulate matter air pollution and cardiovascular disease: an update to the scientific statement from the American Heart Association. *Circulation*. 2010;121:2331–2378.
2. Pope CA 3rd, Burnett RT, Thurston GD, Thun MJ, Calle EE, Krewski D, Godleski JJ. Cardiovascular mortality and long-term exposure to particulate air pollution: epidemiological evidence of general pathophysiological pathways of disease. *Circulation*. 2004;109:71–77.
3. Araujo J. Particulate air pollution, systemic oxidative stress, inflammation, and atherosclerosis. *Air Qual Atmos Health*. 2011;4:79–93.
4. Suwa T, Hogg JC, Quinlan KB, Ohgami A, Vincent R, van Eeden SF. Particulate air pollution induces progression of atherosclerosis. *J Am Coll Cardiol*. 2002;39:935–942.
5. Sun Q, Wang A, Jin X, Natanzon A, Duquaine D, Brook RD, Aguinaldo JG, Fayad ZA, Fuster V, Lippmann M, Chen LC, Rajagopalan S. Long-term air pollution exposure and acceleration of atherosclerosis and vascular inflammation in an animal model. *JAMA*. 2005;294:3003–3010.
6. Araujo JA, Barajas B, Kleinman M, Wang X, Bennett BJ, Gong KW, Navab M, Harkema J, Sioutas C, Lusis AJ, Nel AE. Ambient particulate pollutants in the ultrafine range promote early atherosclerosis and systemic oxidative stress. *Circ Res*. 2008;102:589–596.
7. Araujo JA, Nel AE. Particulate matter and atherosclerosis: role of particle size, composition and oxidative stress. *Part Fibre Toxicol*. 2009;6:24.
8. Yin F, Ramanathan G, Zhang M, Araujo JA. Prooxidative effects of ambient pollutant chemicals are inhibited by HDL. *J Biochem Mol Toxicol*. 2013;27:172–183.
9. Bai N, Kido T, Suzuki H, Yang G, Kavanagh TJ, Kaufman JD, Rosenfeld ME, van Breemen C, Eeden SF. Changes in atherosclerotic plaques induced by inhalation of diesel exhaust. *Atherosclerosis*. 2011;216:299–306.
10. Campen MJ, Lund AK, Knuckles TL, Conklin DJ, Bishop B, Young D, Seilkop S, Seagrave J, Reed MD, McDonald JD. Inhaled diesel emissions alter atherosclerotic plaque composition in ApoE(-/-) mice. *Toxicol Appl Pharmacol*. 2010;242:310–317.
11. Gordon T, Castelli WP, Hjortland MC, Kannel WB, Dawber TR. High density lipoprotein as a protective factor against coronary heart disease. The Framingham Study. *Am J Med*. 1977;62:707–714.
12. Briel M, Ferreira-Gonzalez I, You JJ, et al. Association between change in high density lipoprotein cholesterol and cardiovascular disease morbidity and mortality: systematic review and meta-regression analysis. *BMJ*. 2009;338:b92.
13. Ansell BJ, Navab M, Hama S, Kamranpour N, Fonarow G, Hough G, Rahmani S, Mottahedeh R, Dave R, Reddy ST, Fogelman AM. Inflammatory/antiinflammatory properties of high-density lipoprotein distinguish patients from control subjects better than high-density lipoprotein cholesterol levels and are favorably affected by simvastatin treatment. *Circulation*. 2003;108:2751–2756.
14. Voight BF, Peloso GM, Orho-Melander M, et al. Plasma HDL cholesterol and risk of myocardial infarction: a mendelian randomisation study. *Lancet*. 2012;380:572–580.
15. Khera AV, Cuchel M, de la Llera-Moya M, Rodrigues A, Burke MF, Jafri K, French BC, Phillips JA, Mucksavage ML, Wilensky RL, Mohler ER, Rothblat GH, Rader DJ. Cholesterol efflux capacity, high-density lipoprotein function, and atherosclerosis. *N Engl J Med*. 2011;364:127–135.
16. Patel PJ, Khera AV, Jafri K, Wilensky RL, Rader DJ. The anti-oxidative capacity of high-density lipoprotein is reduced in acute coronary syndrome but not in stable coronary artery disease. *J Am Coll Cardiol*. 2011;58:2068–2075.
17. Navab M, Imes SS, Hama SY, Hough GP, Ross LA, Bork RW, Valente AJ, Berliner JA, Drinkwater DC, Laks H. Monocyte transmigration induced by modification of low density lipoprotein in cocultures of human aortic wall cells is due to induction of monocyte chemotactic protein 1 synthesis and is abolished by high density lipoprotein. *J Clin Invest*. 1991;88:2039–2046.
18. Mackness MI, Arrol S, Abbott C, Durrington PN. Protection of low-density lipoprotein against oxidative modification by high-density lipoprotein associated paraoxonase. *Atherosclerosis*. 1993;104:129–135.
19. Møller P, Loft S. Oxidative damage to DNA and lipids as biomarkers of exposure to air pollution. *Environ Health Perspect*. 2010;118:1126–1136.
20. Patrignani P, Tacconelli S. Isoprostanes and other markers of peroxidation in atherosclerosis. *Biomarkers*. 2005;10:S24–S29.
21. Proudfoot JM, Barden AE, Loke WM, Croft KD, Puddey IB, Mori TA. HDL is the major lipoprotein carrier of plasma F2-isoprostanes. *J Lipid Res*. 2009;50:716–722.
22. Niki E, Yoshida Y, Saito Y, Noguchi N. Lipid peroxidation: mechanisms, inhibition, and biological effects. *Biochem Biophys Res Commun*. 2005;338:668–676.
23. Yoshida Y, Niki E. Bio-markers of lipid peroxidation in vivo: hydroxyoctadecadienoic acid and hydroxycholesterol. *Biofactors*. 2006;27:195–202.
24. Forte TM, Subbanagounder G, Berliner JA, Blanche PJ, Clermont AO, Jia Z, Oda MN, Krauss RM, Bielicki JK. Altered activities of anti-atherogenic enzymes LCAT, paraoxonase, and platelet-activating factor acetylhydrolase in atherosclerosis-susceptible mice. *J Lipid Res*. 2002;43:477–485.
25. Jaouad L, Milochevitch C, Khalil A. PON1 paraoxonase activity is reduced during HDL oxidation and is an indicator of HDL antioxidant capacity. *Free Radic Res*. 2003;37:77–83.
26. Ferretti G, Bacchetti T, Busni D, Rabini RA, Curatola G. Protective effect of paraoxonase activity in high-density lipoproteins against erythrocyte membranes peroxidation: a comparison between healthy subjects and type 1 diabetic patients. *J Clin Endocrinol Metab*. 2004;89:2957–2962.
27. Navab M, Hama SY, Cooke CJ, Anantharamaiah GM, Chaddha M, Jin L, Subbanagounder G, Faull KF, Reddy ST, Miller NE, Fogelman AM. Normal high density lipoprotein inhibits three steps in the formation of mildly oxidized low density lipoprotein: step 1. *J Lipid Res*. 2000;41:1481–1494.
28. Shao B, Pennathur S, Pagani I, Oda MN, Witztum JL, Oram JF, Heinecke JW. Modifying apolipoprotein A-I by malondialdehyde, but not by an array of other reactive carbonyls, blocks cholesterol efflux by the ABCA1 pathway. *J Biol Chem*. 2010;285:18473–18484.
29. Gong KW, Zhao W, Li N, Barajas B, Kleinman M, Sioutas C, Horvath S, Lusis AJ, Nel A, Araujo JA. Air-pollutant chemicals and oxidized lipids exhibit genome-wide synergistic effects on endothelial cells. *Genome Biol*. 2007;8:R149.

Downloaded from http://atvb.ahajournals.org/ by guest on December 26, 2016

30. Tong H, Cheng WY, Samet JM, Gilmour MI, Devlin RB. Differential cardiopulmonary effects of size-fractionated ambient particulate matter in mice. *Cardiovasc Toxicol*. 2010;10:259–267.
31. Kampfrath T, Maiseyeu A, Ying Z, et al. Chronic fine particulate matter exposure induces systemic vascular dysfunction via NADPH oxidase and TLR4 pathways. *Circ Res*. 2011;108:716–726.
32. Suzuki M, Pritchard DK, Becker L, Hoofnagle AN, Tanimura N, Bammler TK, Beyer RP, Bumgarner R, Vaisar T, de Beer MC, de Beer FC, Miyake K, Oram JF, Heinecke JW. High-density lipoprotein suppresses the type I interferon response, a family of potent antiviral immunoregulators, in macrophages challenged with lipopolysaccharide. *Circulation*. 2010;122:1919–1927.
33. Zhu Y, Hinds WC, Kim S, Shen S, Sioutas C. Study of ultrafine particles near a major highway with heavy-duty diesel traffic. *Atmospheric Environment*. 2002;36:4323–4335.
34. Zhu Y, Pudota J, Collins D, Allen D, Clements A, DenBleyker A, Fraser M, Jia Y, McDonald-Buller E, Michel E. Air pollutant concentrations near three Texas roadways, part I: ultrafine particles. *Atmos Environ*. 2009;43:4513–4522.
35. Morawska L, Ristovski Z, Jayaratne ER, Keogh DU, Ling X. Ambient nano and ultrafine particles from motor vehicle emissions: characteristics, ambient processing and implications on human exposure. *Atmos Environ*. 2008;42:8113–8138.
36. Lingard JJ, Agus EL, Young DT, Andrews GE, Tomlin AS. Observations of urban airborne particle number concentrations during rush-hour conditions: analysis of the number based size distributions and modal parameters. *J Environ Monit*. 2006;8:1203–1218.
37. Miller KA, Siscovick DS, Sheppard L, Shepherd K, Sullivan JH, Anderson GL, Kaufman JD. Long-term exposure to air pollution and incidence of cardiovascular events in women. *N Engl J Med*. 2007;356:447–458.

Significance

Exposure to air pollution leads to significant cardiopulmonary health effects resulting in increased cardiovascular morbidity and mortality. Motor vehicle emissions are major pollutants in urban settings. This study shows that hyperlipidemic apolipoprotein E null mice, prone to develop atherosclerosis, exhibited the generation of dysfunctional pro-oxidant and proinflammatory high-density lipoproteins (HDL), when subjected to diesel exhaust emissions for 2 weeks. Mice also exhibited increased susceptibility for the oxidation of non-HDL lipoproteins and greater lipid oxidation in the bronchoalveolar compartment of the lung, circulating blood, and systemic tissues, such as the liver. Several markers of lipid peroxidation in the blood and the liver strongly correlated with the degree of HDL dysfunction, indicating that the loss of HDL cardioprotective properties was associated with markers of systemic oxidation. This is important because the generation of dysfunctional HDL may be one of the mechanisms how air pollutants exacerbate heart disease and strokes in humans.

Downloaded from http://atvb.ahajournals.org/ by guest on December 26, 2016

Arteriosclerosis, Thrombosis, and Vascular Biology

Journal of the American Heart Association

Downloaded from http://atvb.ahajournals.org/ by guest on December 26, 2016

Diesel Exhaust Induces Systemic Lipid Peroxidation and Development of Dysfunctional Pro-Oxidant and Pro-Inflammatory High-Density Lipoprotein

Fen Yin, Akeem Lawal, Jerry Ricks, Julie R. Fox, Tim Larson, Mohamad Navab, Alan M. Fogelman, Michael E. Rosenfeld and Jesus A. Araujo

Arterioscler Thromb Vasc Biol. 2013;33:1153-1161; originally published online April 4, 2013;
doi: 10.1161/ATVBAHA.112.300552
Arteriosclerosis, Thrombosis, and Vascular Biology is published by the American Heart Association, 7272 Greenville Avenue, Dallas, TX 75231
Copyright © 2013 American Heart Association, Inc. All rights reserved.
Print ISSN: 1079-5642. Online ISSN: 1524-4636

The online version of this article, along with updated information and services, is located on the World Wide Web at:
http://atvb.ahajournals.org/content/33/6/1153

Data Supplement (unedited) at:
http://atvb.ahajournals.org/content/suppl/2013/04/04/ATVBAHA.112.300552.DC1.html

Permissions: Requests for permissions to reproduce figures, tables, or portions of articles originally published in *Arteriosclerosis, Thrombosis, and Vascular Biology* can be obtained via RightsLink, a service of the Copyright Clearance Center, not the Editorial Office. Once the online version of the published article for which permission is being requested is located, click Request Permissions in the middle column of the Web page under Services. Further information about this process is available in the Permissions and Rights Question and Answer document.

Reprints: Information about reprints can be found online at:
http://www.lww.com/reprints

Subscriptions: Information about subscribing to *Arteriosclerosis, Thrombosis, and Vascular Biology* is online at:
http://atvb.ahajournals.org//subscriptions/

Supplemental Material

Diesel Exhaust Induces Systemic Lipid Peroxidation and Development of Dysfunctional Pro-oxidant and Pro-inflammatory HDL

Fen Yin, PhD[1]; Akeem Lawal, PhD[1]; Jerry Ricks, BS[2]; Julie R. Fox, PhD[2]; Tim Larson, PhD[2,3]; Mohamad Navab, PhD[1]; Alan M. Fogelman, MD[1]; Michael E. Rosenfeld, PhD[2]; Jesus A. Araujo, MD PhD[1]

From the Department of Medicine, Division of Cardiology, David Geffen School of Medicine, University of California, Los Angeles, CA [1], the Department of Environmental and Occupational Health Sciences, University of Washington, Seattle, WA [2] and the Department of Civil and Environmental Engineering, University of Washington, Seattle, WA [3]

Short title: Diesel Exhaust and HDL Function

Supplemental Tables

Supplemental Table I. Plasma lipids [a]

	Total cholesterol (mg/dl)	HDL cholesterol (mg/dl)	non-HDL cholesterol (mg/dl)
FA	402±37	35±4	371±26
DE	396±24	38±3	356±18
DE+FA	456±41	30±5	411±45

[a] Results are expressed as mean ± SEM. n=8 for each group

Supplemental Table II. Lung levels of HETEs and HODEs

	FA	DE	DE+FA
Lung (ng/ tissue)			
5-HETE	60.9±6.8	26.3±3.6**	43.0±8.1
12-HETE	23220.7±3118.4	21062.4±2143.5	27119.3±2522.5
15-HETE	739.4±65.8	546.1±27.5*	599.6±48.8
9-HODE	4031.9±658.5	4124.4±191.6	3649.3±613.7
13-HODE	4654.9±723.3	4316.1±196.9	4553.1±728.3

Results are expressed as mean ± SEM. n=6 for each group, samples correspond to Experiment 1. * $p < 0.05$ vs FA group. ** $p < 0.005$ vs FA group.

Supplemental Table III. Primers

Gene	Forward	Reverse
GCL-C [a]	AGAAGGGGGAGAGGACAAAC	AGTGATGGTGCAGAGAGCCT
NQO1[a]	TTCTCTGGCCGATTCAGAGT	GGCTGCTTGGAGCAAAATG
ATF4 [a]	ATGATGGCTTGGCCAGTG	CCATTTTCTCCAACATCCAATC
SOD [a]	CTTCTCGTCTTGCTCTCTCTGG	TCCTGTAAATTTGTCCTGACAACA
Alox-5 [b]	GGCACGGCAAAAACAGTATC	TGGCATTTGGCATCAATACTC
Alox-12 [b,]	CATGCCCAGGACAGAGGA	CACACATGGTGAGGAAATGG
Alox-15 [b]	GGGGATGGAGAAGCTACAGG	TCCGCTTCAAACAGAGTGC
PON-1 [b]	GCATCTGAAAACCATCACACA	AAGCTCTCAGGTCCAATAGCA
GPX6 [b]	CTGTGGCCTGACAGCTACG	AAAACCGTGACGTTGAATGG
β-actin [a]	AGCCATGTACGTAGCCATC	CTCTCAGCTGTGGTGGTGA
β-actin [b]	TAGCAGGATGCAGAAGAAGA	CGCTCAGGAGCAATG

[a] Q-PCR was determined using Sybr Green. [b] Q-PCR was done using mouse Universal library probes (Roche).

Supplemental Figures

Supplemental Figure I. FPLC profile of plasma lipoproteins

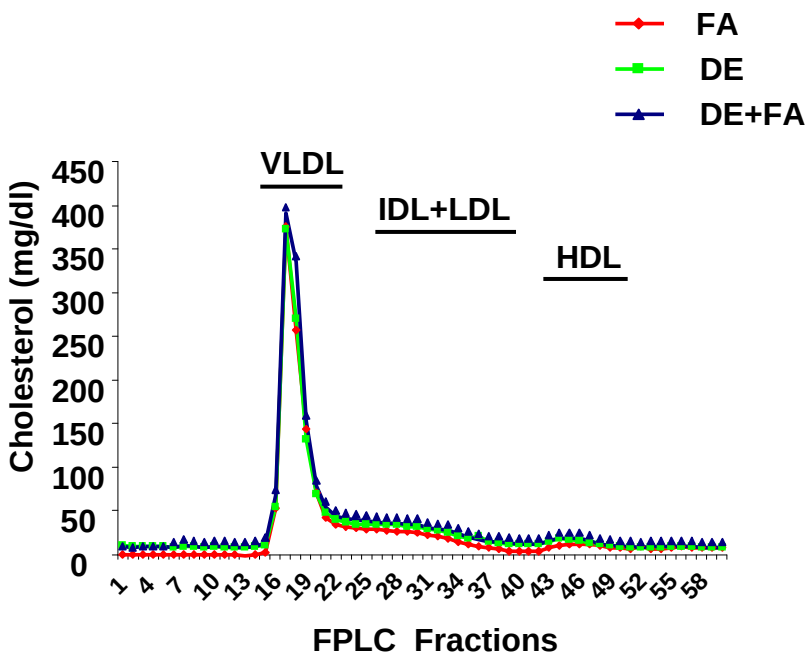

Supplemental Figure I. Mouse plasma (200μl) was applied to two Superose 6 columns in series. Fractions were collected and cholesterol was measured by an enzymatic assay as described in the Supplemental Materials and Methods.

Supplemental Figure II. Reverse Cholesterol Transport

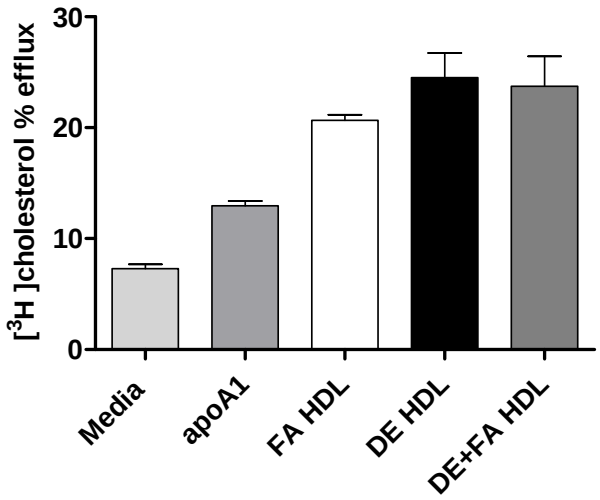

Supplemental Figure II. Cholesterol efflux was determined in duplicate wells of J774 cells, loaded with ^{3}H cholesterol overnight and incubated with HDL 20 µg/ml for 4 hours, apoA1 25 µg/ml or media alone. The degree of efflux is expressed as the mean ± SEM radioactivity in the media divided by the sum of radioactivity in the media plus the cells (x100). HDL was prepared by ultracentrifugation as indicated in the Materials and Methods in animals from the FA (n=3 pools made of 6 individual mice), DE (n=4 individual mice) and DE+FA (n=3 individual mice) from experiment 1. There was no significant difference among HDL from the various mouse groups.

Supplemental Figure III. Myeloperoxidase activity of blood leukocytes

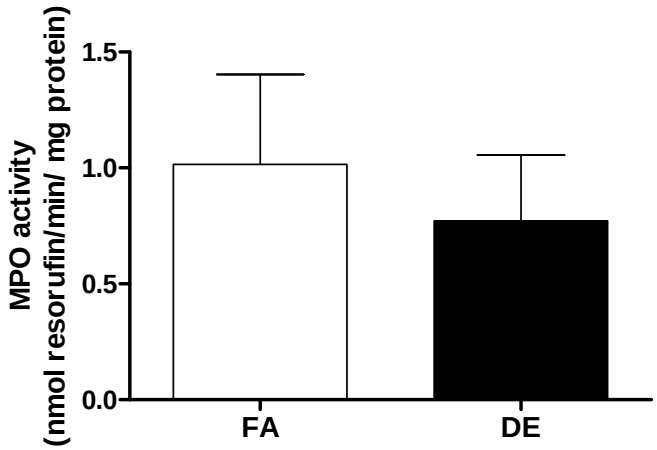

Supplemental Figure III. Myeloperoxidase **(**MPO) activities are expressed as the mean ± SEM in blood leukocytes from FA (n=6) and DE (n=6). Samples correspond to Experiment 2.

Supplemental Figure IV. Liver PON1 and lipoxygenases mRNA expression

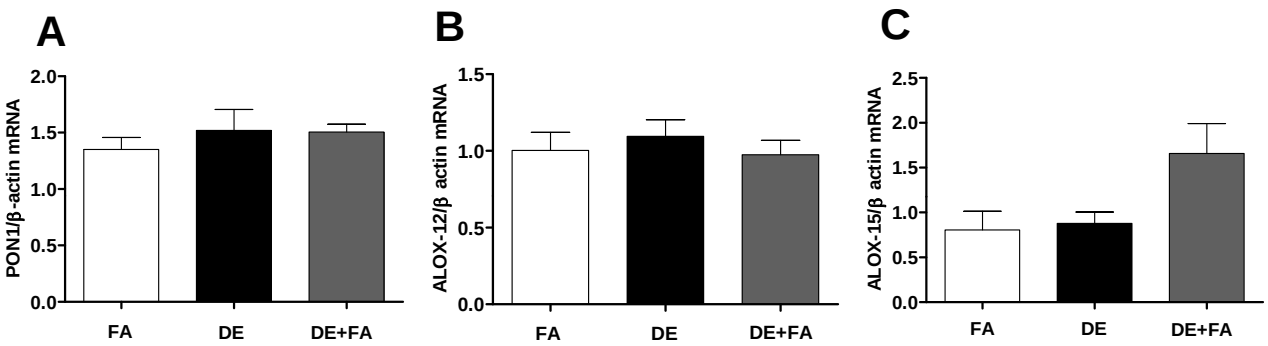

Supplemental Figure IV. Gene expression levels were determined by quantitative PCR in the livers of FA, DE and DE+FA mice. Values are expressed as the mean ± SEM of mRNA levels normalized by β-actin mRNA. Five samples per group were assayed in triplicate. A) PON1: Paraoxonase 1. B) ALOX-12: arachidonate 12-lipoxygenase, C) ALOX -15: arachidonate 15-lipoxygenase. DE+FA mice were not significantly different to FA or DE mice (p=0.1). Samples correspond to experiment 1.

Supplemental Figure V. DE exposure increases oxidizability of apoB-rich lipoproteins.

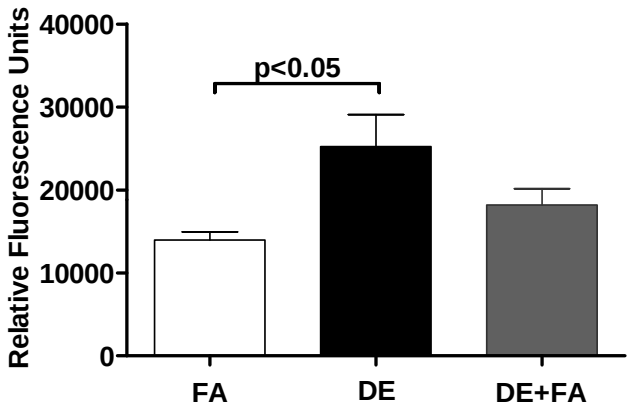

Supplemental Figure V. Oxidation of ApoB containing lipoproteins by air was assessed by DCF fluorescence as described in Supplemental Materials and Methods. Values are expressed as the mean ± SEM of DCF relative fluorescence units in plasma samples from FA (n=11), DE (n=10) and DE+FA (n=10). Samples correspond to experiment 1.

Materials and Methods

Diesel Exhaust Induces Systemic Lipid Peroxidation and

Development of Dysfunctional Pro-oxidant and Pro-inflammatory HDL

Fen Yin, PhD[1]; Akeem Lawal, PhD[1]; Jerry Ricks, BS[2]; Julie R. Fox, PhD[2];
Tim Larson, PhD[2,3]; Mohamad Navab, PhD[1]; Alan M. Fogelman, MD[1];
Michael E. Rosenfeld, PhD[2]; Jesus A. Araujo, MD PhD[1]

From the Department of Medicine, Division of Cardiology, David Geffen School of Medicine, University of California, Los Angeles, CA [1], the Department of Environmental and Occupational Health Sciences, University of Washington, Seattle, WA [2] and the Department of Civil and Environmental Engineering, University of Washington, Seattle, WA [3]

Short title: Diesel Exhaust and HDL Function

Corresponding author: Jesus A. Araujo, MD, PhD. UCLA Division of Cardiology, 10833 Le Conte Avenue, CHS 43-264, Los Angeles, CA 90095. P.O. Box 951679. Phone number (310) 825-3222, Fax number (310) 206-9133. E-mail address: JAraujo@mednet.ucla.edu

DE exposure system

Diesel exhaust (DE) was generated in the exposure facility with a Yanmar America Corp. single cylinder diesel engine generator set with a maximum electrical power output of 5.5 kW (Model YDG5500EV-6EI). The diesel fuel combusted in the generator was ultra low sulfur highway-grade number 2, which is obtained from local distributors. Chevron Grade SAE 15W-40 motor oil was used for lubricating oil. A Simplex Swift-E FT load bank provided a resistive load on the generator that was maintained at 82%. The DE dilution system consisted of a two-step dilution process with overall dilution of 1:380 with heated and humidified air. The DE is aged for ~5 minutes in order to mimic DE aging in the atmosphere. All dilution air for the system was passed through HEPA and carbon filters, permitting a filtered air control exposure option with very low particulate and gaseous organic pollutant levels. The mass concentration was monitored during exposures with a TEOM analyzer (Rupprecht & Patashnick Model 1400a) and an integrating light-scattering nephelometer (Radiance Research Model 903) [1]. For experiment 1, exposures were between 8/30/10 and 11/5/10, the average $PM_{2.5}$ concentration measured was 258 $\mu g/m^3$ (SD 39). In experiment 2 (exposures between 10/17/11 and 11/1/11), the average $PM_{2.5}$ concentration was 253 $\mu g/m^3$ (SD 5).

The following selected exposure characteristics were measured with the DE generated under the same conditions within the human exposure room of the exposure facility with an average $PM_{2.5}$ mass concentration of 216 $\mu g/m^3$ (SD 10). The mass median aerodynamic diameter (MMAD) was 77 (GSD 7.4), obtained by gravimetric analysis of samples collected with a micro orifice uniform deposit impactor (MOUDI, MSP Model 110-NR). The mass distribution is shown in Figure 1B. The average particle number concentration was 145,000 particles/cm^3 (SD 5400), measured with a P-Trak Ultrafine Particle Counter, Model 8525, with specified collection of particle diameters >20 nm. The mass fraction of particle-bound polycyclic aromatic hydrocarbons (PAH) was 21 ng/μg $PM_{2.5}$ (SD 2), measured with an Ecochem PAS 2000. The ratio of the organic carbon to elemental carbon mass concentration was 0.10 (SD 0.02), based on quartz filter samples adjusted with a concurrent dynamic blank; samples were analyzed by Sunset Laboratories using the IMPROVE A thermo optical reflectance method. Oxides of nitrogen concentrations were 1220 ppb NO (SD 160) and 45 ppb NO_2 (SD 17) measured using a Thermo Scientific Model 42C analyzer. The concentration of carbon monoxide was 1.3 ppm (SD 0.1), measured using a Langan analyzer, Model T15n.

Animals and exposure protocol

$ApoE^{-/-}$ (C57BL/6J background) male mice (originally obtained from The Jackson Laboratory, Bar Harbor, ME) were bred in the University of Washington South Lake Union animal facility. The mice were housed in a temperature- and humidity-controlled environment with a 12-h light/dark cycle. Mice were allowed access to water and standard rodent chow during non-exposure periods. At ~ 8 weeks of age, the mice were kept in standard mouse cages and moved into a self enclosed “Biozone” facility connected to the DE generating system. DE exposures were controlled by opening or closing a valve to the “Biozone” resulting in minimal stress for animals during the exposure period. Two exposure experiments were performed (Figure 1A). Experiment 1 consisted in mice assigned to three experimental groups (n=12-13/group) that were exposed to: A) DE for 2 weeks (DE group, n= 12), B) Filtered air for 2 weeks as controls (FA, n=13), and C) DE for 2 weeks followed by FA for 1 additional week (DE+FA, n= 13). Experiment 2 consisted in mice assigned to two experimental groups (n = 10-12/group), exposed to almost identical conditions as groups A (n = 10) and B (n= 12) of experiment 1. Exposures were started after a 7-day period of acclimatization in the “Biozone” and consisted in sessions of 6 hours/day (9 am to 3 pm), 5 sessions/week. DE was titrated to

achieve a concentration of ~ 250 μg/m^3 $PM_{2.5}$ as indicated in the DE exposure system section. Prior to any exposures and immediately following the last exposure session, blood was drawn from the retro-orbital sinus of each mouse into heparin containing tubes and centrifuged (300 x g) to generate plasma. In experiment 2, mice were euthanized with an overdose of inhaled isoflurane immediately after retro-orbital bleeding. The trachea was isolated and cannulated to allow the lungs to be lavaged with 1.0 ml PBS, two times. The lavage fluid was centrifuged at 250 x g for 10 minutes at 4°C. The resulting supernatant was immediately stored at -80ºC for subsequent analysis of HETEs/HODEs and total protein. Animal procedures were approved by the Animal Care and Use Committee of the University of Washington.

Plasma Lipoproteins and separation by dextran sulfate precipitation

Human LDL (hLDL) and human HDL (hHDL) were obtained from healthy donors at the UCLA Division of Cardiology. Human LDL was prepared by ultracentrifugation [2] or by FPLC [3] in the assessment of anti-oxidant and anti-inflammatory capacities, respectively. Human HDL and test mouse HDLs were prepared by dextran sulfate precipitation or FPLC in the assessment of HDL anti-oxidant and anti-inflammatory capacities, respectively. All mouse plasma samples were cryo-preserved in sucrose prior to use as described [4]. For the dextran sulfate precipitation, apoB-containing particles were precipitated from plasma by dextran sulfate via adding 10μl of LipiDirect Magnetic HDL cholesterol precipitating reagent (Reference Diagnostics, Inc, Bedford, MA) to 50μl of plasma. This mixture was incubated at room temperature for 10 min, then centrifuged at 12,000 rpm for 15 min at 4° C. The supernatant, containing the HDL fraction, was removed and cholesterol was quantified using a colorimetric assay (Thermo Scientific, Middletown, VA, USA). This HDL fraction was used in the assessment of anti-oxidant capacity (Figures 2B&C). The precipitated pellet was also dissolved in Tris-HCl (pH7.4) buffer and centrifuged at 12,000rpm for 15 min at 4 $^{\circ}$C. The supernatant, containing ApoB-rich lipoproteins, was collected and used for the oxidizability assay (Supplemental Figure V).

Separation of plasma lipoproteins by fast performance liquid chromatography (FPLC) and ultracentrifugation

Plasma lipoproteins FPLC profile shown in Supplemental Figure I was obtained using mouse plasmas with a AKTA purifier system FPLC equipped with a Superose^{TM}6,10/300 column. (GE Healthcare, Pittsburgh, PA, USA). The elution was performed in 0.15 M NaCl, 0.01 M Na_2HPO4, pH 7.5, 0.02% NaN_3 as a running buffer. After loading 150 μl plasma, the system was run with a constant flow rate of 0.5 ml/min. Set the fraction collector for 0.5 ml/tube. Discarded the first 12 fractions (6ml) and started collecting from fraction numbers 13 to 72 (i.e. 60 fractions are collected). Fractions containing the plasma lipoproteins were used for further analysis to determine cholesterol levels of each fraction. The cholesterol (Thermo Scientific, Pittsburgh, PA, USA) determination assays are standard enzymatic, colorimetric methods. Plasma lipoproteins were also separated by ultracentrifugation as described by us [5], using a D_2O/sucrose lipoprotein separation ultracentrifugation methodology, based on minor modifications of the previously reported technique [6]. Briefly, 0.2ml of plasma with an adjusted density of 1.019 g/ml was added to the polycarbonate tubes (Cat #: 343776, Beckman Coulter, Palo Alto, CA), the upper fraction with density less than 1.019 g/ml, mainly containing VLDL was carefully withdrawn with a Pasteur pipette after a 2.5 h ultracentrifugation at 495,000 g with TLA 120.1 rotor in an optima^{TM} MAX-XP ultracentrifuge at 16°C. The density of bottom fraction containing LDL and HDL was adjusted to 1.063 g/ml and the volume was brought up to 0.4 ml. The upper fraction containing LDL with the density of 1.019–1.063 g/ml was obtained after centrifugation at 495,000 g for 3 h at 16°C. 0.2 ml of the bottom fraction with adjusted density of 1.210 g/ml and final volume of 0.4 ml, was centrifuged at 495,000 g for 16 h at 12°C to recover the upper fraction with density of 1.063–1.210 g/ml (HDL). HDL separated by ultracentrifugation was used in the cholesterol efflux assays (Supplemental Figure II).

Assessment of HDL anti-oxidant capacity

We used a cell-free assay as reported in details by us [5]. Briefly, Dichlorofluorescein diacetate (DCF-DA, Sigma-Aldrich, St. Louis, MO) stock solution was prepared in fresh methanol at 2.0 mg/ml and stored at -80 ºC protected from light. Prior to each experiment, 1 ml of 0.1 M NaOH was added to 250 µl of stock DCF-DA and incubated at room temperature while protected from light for 30 min. The reaction was stopped by neutralizing the solution with 8.75 ml of 0.1 M phosphate buffered saline (PBS). This results in the conversion of DCF-DA to dihydrodichlorofluorescein (DCFH). Upon oxidation, DCFH transforms into DCF. We evaluated HDL anti-oxidant capacity by assessing its ability to inhibit LDL oxidation by air, measured by DCF fluorescence. The change in fluorescence intensity is the result of the oxidation of DCFH induced by free radicals generated in the oxidation of human LDL (hLDL) in the absence or presence of the test HDL. 12.5 µl of human LDL (50µg cholesterol/ml) was mixed with 12.5 µl of test mouse HDL (50µg cholesterol/ml), and 75 µl of Tris-HCL buffer (pH7.4) in black, flat bottom polystyrene microtiter plates and incubated at 37°C for 60 min. 25 µl of DCFH solution (50µg /ml) was then added to each well, mixed, and incubated at 37°C for 2h. 12.5 µl of human HDL (hHDL, 50µg cholesterol/ml) were used as a positive control for test mouse HDL. hLDL was prepared by ultracentrifugation [2]. hHDL and test mouse HDLs were prepared by dextran sulfate precipitation as described above. Fluorescence intensity was determined with a plate reader (SynergyMx, BioTek, Vermont, USA) at an excitation wavelength of 485 nm, emission wavelength of 530 nm. A sensitivity level slit width of 9 nm was used for excitation and emission, the intra- and inter-assay CVs were 2.2 and 6.4, respectively. The DCF fluorescence data was converted into an HDL oxidant index (HOI) that equals the ratio of fluorescence in the presence of HDL divided by the fluorescence in the absence of HDL. An index < 1.0 denotes protective anti-oxidant HDL, while an index > 1.0 denotes pro-oxidant HDL.

Assessment of HDL anti-inflammatory capacity

We used a Monocyte Chemotaxis Assay (MCA) that evaluates the protective capacity of HDL against LDL-induced monocyte chemotactic activity as previously described [7] . Monocytes were isolated from blood obtained from a large pool of healthy donors at the UCLA Division of Cardiology, Atherosclerosis Research Unit under a protocol approved by the Human Research Subject Protection Committee of the University of California, Los Angeles (Los Angeles, CA). Human aortic endothelial cells (HAEC) and human aortic smooth muscle cells (SMC) were isolated from trimmings of fresh surgical aortic specimens from normal donor hearts during transplantation under a protocol approved by the Human Research Subject Protection Committee of the University of California, Los Angeles (Los Angeles, CA). Co-cultures of HAEC and SMC were treated for 18 hours with a standard source of human LDL (100 µg LDL cholesterol/ml), in the absence or presence of a standard source of human LDL (hLDL) or test mouse HDL (50 µg HDL cholesterol/ml). Human HDL (hHDL) was used as a positive control for the test mouse HDL. LDL and both human and test mouse HDLs were separated by FPLC [3]. Cells were then washed and incubated in fresh culture medium for 8 hours, following which supernatants were collected to assess monocyte chemotactic activity after 40-fold dilution, which was expressed as the number of monocytes that have transmigrated per high power field (HPF) [3].

Assessment of oxidizability of apoB-containing lipoproteins

ApoB-containing lipoproteins were precipitated from plasma with the use of LipiDirect Magnetic HDL cholesterol precipitating reagent as indicated above. Precipitated ApoB-containing pellets were dissolved in 100 µl of 40mM Tris-HCl (pH 7.4) buffer, vortexed, and centrifuged at 12,000 rpm, 4°C for 10 min. The supernatant, enriched in LDL and VLDL fractions, was used to assess oxidizability by air, measured by DCF fluorescence. The supernatant cholesterol concentrations

were adjusted to 5 µg/ml by adding Tris-HCl buffer (ph 7.4) to a total volume of 150 µl, which were then transferred to black, flat bottom polystyrene microtiter plates, and incubated at 37°C for 60 min. 25 µl of DCFH solution (50µg /ml) was then added to each well, mixed, and incubated at 37°C for 2h. Fluorescence intensity was determined with a plate reader (SynergyMx, BioTek, Vermont, USA) at an excitation wavelength of 485 nm, emission wavelength of 530 nm.

Myeloperoxidase (MPO) activity

Leukocytes (were isolated from blood with Lympholyte-poly reagent as per the manufacturer instructions (CEDARLANE LABORATORIES LIMITED, Hornby, Ontario, Canada). Neutrophil MPO activity was determined with a fluorescence kit as per the manufacturer instructions (Cayman Chemical Company, Ann Arbor, MI, USA).

Paraoxonase Activity

The rate of hydrolysis of paraoxon was measured as described by Eckerson et al. [8] with some modifications. Briefly, 1.0-mM paraoxon (Sigma-Aldrich), freshly prepared in 195 µL of 50-mM glycine buffer containing 1-mM calcium chloride (pH 10.5) was incubated at 37°C with 5 µL of serum for 10 minutes in 96 well plates. Formation of p-nitrophenol was monitored at 412 nm and activity was expressed as µmol p-nitrophenol/L/plasma/min.

Plasma 8-isoprostane levels

Plasma 8-isoprostane levels were determined with an ELISA kit as per the manufacturer instructions (Cayman Chemical Company, Ann Arbor, MI, USA).

Assessment of liver and lung MDA levels

Snap frozen liver (50-70 mg) or lung tissue samples (70-90mg) were homogenized with 8× weight of ice-cold 40 mM Tris-HCl buffer (pH 7.4, containing %0.01 BHT). The homogenate was centrifuged at 6,000 × *g* for 15 min at 4°C; the supernatant was taken to determine MDA levels by a colorimetric assay (OxisResearch, OR, USA) as per the manufacturer's instructions. The MDA concentrations were normalized by total protein levels in the homogenates. The protein concentration of tissue homogenates was determined by a BCA™ method (Thermo Scientific, Middletown, VA, USA). A standard curve was used to calculate the concentration (µM/mg protein) of MDA for each sample.

Cholesterol Efflux

Cholesterol efflux assays were performed as previously described [9]. Briefly, J774 cells were cultured in DMEM and 10% FBS. On day 1 of the assay, cells were plated at 50% confluence in 24-well plates. On day 2, the cells were washed and incubated for 24 h in medium A supplemented with an ACAT inhibitor (Oleyl Anilide; 2 µg/ml) and [^{3}H]cholesterol (1.0 µCi/ml). On day 3, the cells were washed twice with PBS and then incubated for 2–4 h in fresh medium, devoid of radiolabeled cholesterol, The cells were rewashed before addition of 0.5 ml medium B (DMEM containing 0.2% BSA) in the absence or presence of different mouse HDL (20 µg/ml) and apoAI (25 µg/ml). After 4 hour incubation, the supernatants were removed and centrifuged at 14,000 × *g* for 10 min and radioactivity content was measured. Cells were washed with PBS, lysed using 0.1N NaOH and assessed for radioactivity content. Radioactivity was determined by liquid scintillation counting in a TRI-CARB 2900TR liquid scintillation counter (Packard Bioscience Company). Cholesterol efflux was determined in duplicate for each condition and efflux of radioactive cholesterol from the cells into the medium was calculated as the radioactivity in the media divided by the sum of radioactivity in cells plus radioactivity in media x 100.

Western immunoblots of mouse liver samples

Snap frozen liver (50-70 mg) samples were homogenized with 8× weight of ice-cold 40 mM Tris-HCl buffer (pH 7.4, containing %0.01 BHT). The homogenate was centrifuged at 6,000 × *g* for 15 min at 4°C. The supernatant was taken and protein concentrations were determined by the BCA method (Thermo Scientific). 40–60 µg of protein lysate were denatured with SDS-reducing buffer by boiling it for 5 min; samples were electrophoresed on a 10% polyacrylamide SDS gel. The separated proteins were transferred to PVDF membranes and probed with rabbit anti-5LOX polyclonal Ab (AB3796, Millipore) followed by incubation with goat anti-actin polyclonal Ab (sc-1616; Santa Cruz, Biotechnology). Reactive proteins were detected using an enhanced chemiluminescence detection system (Amersham, Arlington Heights, IL, USA) according to the manufacturer's procedures. Quantification of the Western blots was performed by densitometric analyses using the ImageJ software.

Plasma and tissue levels of oxidized free fatty acids

a) Chemicals: (±)13-hydroxy-9Z,11E-octadecadienoic acid (13-HODE), (±)9-hydroxy-10E,12E-octadecadienoic acid (9-HODE), (±)15-hydroxy-5Z,8Z,11Z,13E-eicosatetraenoic acid (15-HETE), (±)5-hydroxy-6E,8E,11Z,14Z-eicosatetraenoic acid (5-HETE),15(S)-hydroxy-5Z,8Z,11Z,13E-eicosatetraenoic- 5,6,8,9,11,12,14,15-d8 acid (15(S)-HETE-d8), 13 (S)-hydroxy-9Z,11E-octadecadienoic-9,10,12,13-d4 acid (13 (S)-HODE-d4), were purchased from Cayman Chemicals (Ann Arbor, MI, USA). HPLC grade methanol was obtained from Sigma-Aldrich (St. Louis, MO, USA). HPLC grade acetonitrile was obtained from Fisher Scientific (Pittsburgh, PA, USA). b) Preparation of plasma samples: Samples were prepared as previously described with slight modifications [10]. Briefly, 25µl volume of plasma samples were transferred to a 2 ml polypropylene tube, and spiked with 12.5µl of internal standards mixture (15(S)-HETE-d8, 13(S)-HODE-d4, 50ng/ml each) in methanol. Subsequently, the pH of the samples was adjusted to ~ 3.0 using 450 µl of 0.5% acetic acid. The samples were left for 15 min on ice for complete acidification and equilibration. The resulting sample was loaded onto a preconditioned 1cc Oasis HLB solid-phase extraction (SPE) cartridge (Waters). The SPE cartridge was equilibrated with 1 ml methanol followed by 1 ml water before the sample load. The sample was slowly loaded on the cartridge, and the cartridge was washed with 1ml 5% methanol in water. HETEs/HODEs were eluted with 1 ml methanol. The eluate was then evaporated to dryness under a stream of nitrogen. 61 µl of methanol was added to the dried extract, vortexed for 30s, and the reconstituted extract was centrifuged at 13,200 rpm for 20min at 4 °C to remove any precipitate that could clog the LC/MS/MS instrument. The resulting supernatants were transferred to autosampler vials and processed for LC/MS/MS analysis, the final concentration for internal standards mixture was 10 ng/ml for each. c) Preparation of liver, lung and large intestine tissue samples: Snap frozen liver (50-70 mg), lung tissue samples (70-90mg), large intestine (4cm length, 60-90 mg) were homogenized with 8× weight of ice-cold 40 mM Tris-HCl buffer (pH 7.4, containing %0.02 BHT). The homogenate was centrifuged at 6,000 × g for 15 min at 4°C. The supernatant was transferred to another vial. About 100-µL aliquot of the homogenate (normalized by protein concentration) was subjected to extraction of HETEs/HODEs using the same methodology employed for the plasma samples. d) LC–MS/MS Analysis: LC-MS/MS analysis was performed as previously described [10]. The transitions monitored were mass-to-charge ratio (m/z): 319.0→115.0 for 5-HETE; 319.1→179.0 for 12-HETE; 319.1→219.0 for 15-HETE; 295.0→194.8 for 13-HODE; 295.0→171.0 for 9-HODE; 327.1→226.1 for 15(S)-HETE-d8; 327.1→184.0 for 12(S)-HETE-d8; 299.0 →197.9 for 13(S)-HODE-d4

Gene expression

RNA was harvested and gene expression levels were determined by quantitative PCR (qPCR) as previously described [11]. Briefly, RNA was isolated from liver, lung and aorta using TRIZOL reagent (Invitrogen, Carlsbad, CA). DNase treatment was performed using DNaseI (Invitrogen, Carlsbad, CA). cDNA was synthesized using cDNA Synthesis kit (Applied Biosystems). Primers (Integrated DNA technologies) to mouse cDNA are shown in Supplemental Table II. Quantitative PCR (qPCR) was performed using a LightCycler 480 (Roche Molecular Biochemicals), according to manufacturer's protocols. PCR conditions were: 95ºC for 3 min, 40 cycles of 95ºC for 15 sec, 60ºC for 30 sec and 72ºC for 30 sec. cDNA quantity for each gene was determined using a standard curve constructed from the Cycle thresholds of each dilution sample. To quantify the relative amount of cDNA, a standard curve was constructed based on the Crossing Point (Cp) values of each dilution sample. The Cp values were determined using the second derivative analysis (LightCycler Relative Quantification Software). Samples were then normalized to β-actin quantity measured by qPCR for each sample. For some genes, qPCR reactions were performed using iQ Sybr Green Supermix (Bio-Rad) while for other genes, qPCR reactions were performed using the Universal Probe Library (Roche Molecular Biochemicals) as indicated in Supplemental Table II.

Statistical analysis

All data were expressed as means ± SEM and corresponds to experiment 1 unless indicated otherwise. Comparisons among three groups or more were analyzed by one-way analysis of variance (ANOVA). When statistically significant, post-hoc analysis was performed by Bonferroni. Unpaired two-tailed Student's t-test was employed for comparisons between two groups. We used linear regression and Pearson's r to determine correlations between HOI and various lipid peroxidation products. Differences were considered statistically significant at the p-value of ≤ 0.05.

.

REFERENCES

1. Gould T, Larson T, Stewart J, Kaufman JD, Slater D, McEwen N. A controlled inhalation diesel exhaust exposure facility with dynamic feedback control of PM concentration. *Inhal Toxicol.* 2008;20:49-52.
2. Navab M, Hama SY, Hough GP, Subbanagounder G, Reddy ST, Fogelman AM. A cell-free assay for detecting HDL that is dysfunctional in preventing the formation of or inactivating oxidized phospholipids. *J Lipid Res.* 2001;42:1308-1317.
3. Navab M, Imes SS, Hama SY, Hough GP, Ross LA, Bork RW, Valente AJ, Berliner JA, Drinkwater DC, Laks H, et al. Monocyte transmigration induced by modification of low density lipoprotein in cocultures of human aortic wall cells is due to induction of monocyte chemotactic protein 1 synthesis and is abolished by high density lipoprotein. *J Clin Invest.* 1991;88:2039-2046.
4. Navab M, Hama SY, Anantharamaiah GM, Hassan K, Hough GP, Watson AD, Reddy ST, Sevanian A, Fonarow GC, Fogelman AM. Normal high density lipoprotein inhibits three steps in the formation of mildly oxidized low density lipoprotein: steps 2 and 3. *J Lipid Res.* 2000;41:1495-1508.
5. Yin F, Ramanathan G, Zhang M, Araujo JA. Prooxidative Effects of Ambient Pollutant Chemicals Are Inhibited by HDL. *J Biochem Mol Toxicol.* 2013;27:172-182.
6. Stahlman M, Davidsson P, Kanmert I, Rosengren B, Boren J, Fagerberg B, Camejo G. Proteomics and lipids of lipoproteins isolated at low salt concentrations in D2O/sucrose or in KBr. *J Lipid Res.* 2008;49:481-490.
7. Araujo JA, Barajas B, Kleinman M, Wang X, Bennett BJ, Gong KW, Navab M, Harkema J, Sioutas C, Lusis AJ, Nel AE. Ambient particulate pollutants in the ultrafine range promote early atherosclerosis and systemic oxidative stress. *Circ Res.* 2008;102:589-596.
8. Eckerson HW, Romson J, Wyte C, La Du BN. The human serum paraoxonase polymorphism: identification of phenotypes by their response to salts. *Am J Hum Genet.* 1983;35:214-227.
9. Francis GA, Knopp RH, Oram JF. Defective removal of cellular cholesterol and phospholipids by apolipoprotein A-I in Tangier Disease. *J Clin Invest.* 1995;96:78-87.
10. Imaizumi S, Grijalva V, Navab M, Van Lenten BJ, Wagner AC, Anantharamiah GM, Fogelman AM, Reddy ST. L-4F differentially alters plasma levels of oxidized fatty acids resulting in more anti-inflammatory HDL in mice. *Drug Metab Lett.* 2011;4:139-148.
11. Barajas B, Che N, Yin F, Rowshanrad A, Orozco LD, Gong KW, Wang X, Castellani LW, Reue K, Lusis AJ, Araujo JA. NF-E2-related factor 2 promotes atherosclerosis by effects on plasma lipoproteins and cholesterol transport that overshadow antioxidant protection. *Arterioscler Thromb Vasc Biol.* 2011;31:58-66.